Napabucasin-loaded PLGA nanoparticles trigger anti-HCC immune responses by metabolic reprogramming of tumor-associated macrophages

Zhenwei Song[1], Hongfei Chen[2], Xueyao Wang[1], Zhiyue Zhang[2], Hui Li[2], Huajun Zhao[1], Yang Liu[2], Qiuju Han[1] and Jian Zhang[1*]

Abstract

Background JAK/STAT3 is one of the critical signaling pathways involved in the occurrence and development of hepatocellular carcinoma (HCC). BBI608 (Napabucasin), as a novel small molecule inhibitor of STAT3, has shown previously excellent anti-HCC effects in vitro and in mouse models. However, low bioavailability, high cytotoxicity and other shortcomings limit its clinical application. In this study, PLGA was selected to prepare Napabucasin PLGA nanoparticles (NPs) by solvent evaporation method, overcoming these limitations and improving the passive targeting effect that nanoparticle mediated. Base on this, we systematically evaluated the anti-HCC effect of Napabucasin-PLGA NPs and explored the underlying mechanisms.

Methods Napabucasin-PLGA NPs were prepared by solvent evaporation method. CCK-8 assay, Annexin V/PI double staining, RT-qPCR, colony formation assay, and Western blotting were performed to evaluate the anti-HCC effect of Napabucasin-PLGA NPs in vitro. Proliferation assay and migration assay were used to detect the effects of Napabucasin-PLGA NPs-treated HCC-TAMs on tumor biological characteristics of HCC cells. Flow cytometry was used to detect anti-HCC immune responses induced by Napabucasin-PLGA NPs in vivo.

Results Our results demonstrated that Napabucasin-PLGA NPs could improve the bioavailability of Napabucasin and enhance Napabucasin-mediated the anti-HCC effects in vitro and in vivo with no significant drug toxicity. In addition to the direct inhibitory effects on the tumor biological characteristics of HCC cells, Napabucasin-PLGA NPs could promote the polarization of macrophages from tumor-promoting M2-type to anti-tumor M1-type, improving the tumor immune microenvironment and augmenting T cell-mediated anti-tumor responses. The underlining mechanisms showed Napabucasin-PLGA NPs suppressed the STAT3/FAO signaling axis in HCC-induced tumor-associated macrophages (TAMs).

Conclusions These findings demonstrated Napabucasin-PLGA NPs is a potential therapeutic candidate for HCC, and provided a new theoretical and experimental basis for further development and clinical application of Napabucasin.

Keywords STAT3, Napabucasin, Nanoparticles, TAMs, FAO

*Correspondence:
Jian Zhang
zhangj65@sdu.edu.cn
Full list of author information is available at the end of the article

Song *et al. Journal of Translational Medicine*   (2024) 22:1125

Page 2 of 17

Introduction

Hepatocellular carcinoma (HCC) is one of the most common malignant tumors in the world, with approximately 7.5 million new cases each year and a higher incidence in men than in women [1]. As a malignant tumor of the digestive system, HCC has the characteristics of insidious onset, and most of the patients have entered the advanced stage as diagnosed, making the treatment for HCC more difficult and high recurrence rate. For advanced HCC, sorafenib has been the first-line drug for systemic therapy for more than a decade. However, the clinical efficacy of sorafenib is not satisfactory and only prolong the survival of patients with HCC by 3 months [2]. Therefore, finding effective drugs is crucial for the clinical treatment of HCC.

As a convergence point of many oncogenic signaling pathways, signal transducer and activator of transcription 3 (STAT3) plays a central role in regulating antitumor immune responses. STAT3 inhibits the expression of immune-activating factors and promotes the production of immune-suppressing factors. Numerous studies have shown that overexpression and constitutive activation of STAT3 frequently occur in HCC, which is correlated with poor prognosis of patients with HCC [3, 4]. IL-6 and IL-22 are the main stimulators of STAT3 signaling in HCC cells. Through the transcriptional regulation of target genes, cooperating with NF-κB and epigenetic regulation of miRNAs [5–7], activated STAT3 augments the proliferation, anti-apoptosis, migration, invasion, angiogenesis and stem cell properties of HCC. Therefore, targeting STAT3 signaling pathway has become a therapeutic strategy for many cancers.

Currently, STAT3-targeted inhibitors can be classified into three categories: peptides, small molecule compounds and oligonucleotides [8]. Napabucasin (BBI608), a small molecule inhibitor that selectively target the DNA binding domain of STAT3, is the only one inhibitor of STAT3 that enters phase III trials so far. The results of monotherapy trials show Napabucasin has a potential impact on advanced colorectal cancer [9], and FDA has approved Napabucasin as an orphan drug for the treatment of gastric and pancreatic cancers. However, the clinical effect of Napabucasin on patients with HCC has not been reported. Our previous study showed Napabucasin displayed excellent anti-HCC effects in vitro and in mouse models [10]. Nevertheless, because of the low bioavailability, Napabucasin displays low therapeutic index and high toxicity. Poly lactic-co-glycolic acid (PLGA) is formed by the polymerization of lactic acid and glycolic acid, which can be hydrolyzed to produce lactic acid in vivo. After the tricarboxylic acid (TCA) cycle, PLGA is degraded into water and carbon dioxide. PLGA has been a pharmaceutical excipient approved by FDA.

Over the past few decades, PLGA-based biodegradable microspheres have been widely used in drug delivery, and dozens of products have been approved for clinical application such as cancer treatment [11]. Based on the characteristics of different cancers, the delivery system is designed to improve the target activity and therapeutic effects of drugs, and prolongs the duration of drug action [12–14].

Tumor-associated macrophages (TAMs) are involved in the formation of tumor microenvironment (TME) and widely present in various tumors. TAMs have been demonstrated to be associated with tumor growth, invasion, metastasis and drug resistance [15]. Based on the phenotype and function, TAMs are usually divided into two functional subtypes, namely classically activated M1 macrophages and alternative activated M2 macrophages. Both M1 and M2 macrophages are highly plastic, the former usually exerts pro-inflammatory and anti-tumor functions, while the latter can disturb T cell-mediated anti-tumor immune responses and promote the proliferation, metastasis and angiogenesis of tumor cells [16]. However, TAMs are mainly M2-like phenotype, therefore targeted eliminating M2-type TAMs or reversing M2-type to M1-type TAMs in TME has become a potential strategy for anti-tumor immunotherapy [17]. Noteworthily, STAT3 is constitutively activated in TAMs, and knockout of STAT3 can inhibit the M2 phenotype of TAMs, thereby suppressing the growth of glioma [18]. Thus, targeted inhibiting STAT3 activity in TAMs might activate immune system and promote anti-tumor immune responses.

In order to improve the bioavailability and reduce the toxicity of Napabucasin, in this study, PLGA was selected as carrier material to prepare Napabucasin-loaded nanoparticles. We systemically evaluated the anti-tumor effects of Napabucasin-PLGA NPs on HCC in vitro and in vivo. Furthermore, we analyzed the influence of Napabucasin-PLGA NPs on tumor immune microenvironment, and clarified the relevant mechanism of Napabucasin-PLGA NPs in regulating the polarization and function of TAMs. This study provided a theoretical and experimental basis for the further development and application of Napabucasin-PLGA NPs in the treatment of HCC.

Materials and methods

Cell lines

Human hepatocellular carcinoma cell lines Huh7, Hep3B and mouse hepatocellular carcinoma cell line Hepa1-6, human embryonic kidney cell HEK-293T and mouse monocyte-macrophage leukemia cell line RAW264.7 were purchased from Shanghai Cell Bank (Chinese Academy of Sciences). Huh7, Hepa1-6, HEK-293T

and RAW264.7 cells were cultured in DMEM medium (HyClone), and Hep3B cells were cultured in MEM medium (HyClone). The culture medium was supplemented with 10% fetal bovine serum (Biological Industries, 04-001-1ACS), 100 U/mL penicillin and 100 mg/mL streptomycin. All cells were cultured in the 5% CO_2 incubator at 37 °C.

Preparation of Napabucasin-PLGA NPs

Napabucasin-loaded nanoparticles (Napabucasin-PLGA NPs) were prepared by solvent evaporation method [19]. Briefly, 1 mg Napabucasin (Selleck, 83280-65-3) and 10 mg PLGA (MW, 5000 Da) (Hangzhou Xinqiao Biotechnology Co., LTD) were completely dissolved in 400 μL dichloromethane. This solution was dropped into 5 mL sterile Milli-Q water and stirred at room temperature, and then ultrasonic emulsified for 30 min at low temperature to get a uniform emulsion. After stirring for 12 h to volatilize the dichloromethane, the emulsion was centrifuged at 10,000 rpm for 10 min, and the deposit was Napabucasin PLGA nanoparticles (Napabucasin-PLGA NPs). Meanwhile, non-drug loaded PLGA nanoparticles (Empty NPs) were prepared similarly but without Napabucasin. Endotoxin-free Milli-Q water was used for preparing all the aqueous solutions.

Characterization of Napabucasin-PLGA NPs

The hydrodynamic size of Napabucasin-PLGA NPs was determined by dynamic light scattering (DynaPro NanoStar). The suspension of Napabucasin-PLGA NPs was centrifuged at 10,000 rpm for 10 min, and the supernatant was collected and Napabucasin loading amount in Napabucasin-PLGA NPs was detected by UV–vis spectrophotometer at 235 nm. The deposit of Napabucasin-PLGA NPs and empty NPs were redispersed in sterile Milli-Q water with the final concentration of 1 nM, respectively. The laser pointer was used to verify whether the NPs had the Tyndall effect. The morphology of Napabucasin-PLGA NPs was detected by transmission electron microscopy (TEM). The drug release behavior of Napabucasin-PLGA NPs in vitro was determined by dynamic membrane dialysis method [20], and the concentration of Napabucasin at different time points was measured by UV–vis spectrophotometry. The cumulative release percentage of Napabucasin-PLGA NPs was calculated and the drug releasing curve was drawn.

Animal experiments

Male C57BL/6J mice (5-week-old) were purchased from Beijing HFK Company (Beijing, China). All mice were housed in the specific pathogen-free facility. 1×10^7 Hepa1-6 cells were injected into the left axillary region of the mice, and the body weight and tumor volume were recorded every 2 days. Seven days after inoculation of Hepa1-6 cells, these mice were treated with Napabucasin-PLGA NPs and Napabucasin once every 2 days (*i.p*), respectively. To confirm the role of T cells in Napabucasin-PLGA NPs-induced anti-HCC effects, 200 μg/mouse In vivo mAb anti-mouse CD4 (BE0119, Bio X Cell Company) or In vivo mAb anti-mouse CD8α (BE0061, Bio X Cell Company) was intraperitoneally injected on the day before Napabucasin-PLGA NPs treatment, and Empty NPs was used as control. All animal protocols and experiments conformed to the Institutional Animal Care and Use Committee of Shandong University (19040), China. All animals received humane care, and all operations and experiments were carried out following the Guide for the Care and Use of Laboratory Animals.

RNA extraction and quantitative real-time PCR

Cells were lysed using Trizol reagent (Invitrogen, 15596018), and the total RNA was extracted. Then cDNA was obtained using a reverse transcription kit (CWBIO, CW2569). The primer sequences for PCR are shown in Supplementary Table 1. Real-time fluorescent quantitative PCR (qPCR) was performed using SYBR premix (CWBIO, CW0659S) according to the manufacturer's instructions.

Western blotting analysis

Cells were lysed with RIPA lysate (MedChemExpress, HY-K1001) to obtain total cell protein. Protein concentrations were quantified using the BCA Protein Assay Kit (Beyotime, P0012S). Then protein was added into the equal-volume 2× loading buffer and denatured at 98 °C for 15 min, followed by separating on 10% SDS-PAGE. After electro-transferring to a polyvinylidene fluoride membrane (Millipore, ISEQ00010, Billerica, MA, USA). The flowing antibodies were used to probe target proteins: β-actin (Rabbit, AC038, ABclonal), STAT3 (Mouse, 9139, CST), p-STAT3 (Rabbit, 30835, CST).

Flow cytometry analysis

The tumor tissues were collected and cut into small pieces, and then treated with digestive fluid (100 mL DMEM supplemented with 2 mL FBS, 0.1 g collagenase IV and 50 μL hyaluronidase) at 37 °C for 60 min, and passed through a 74 μm copper mesh. The infiltrating mononuclear cells were obtained by 40% Percoll separation solution. For the detection of cell surface markers, the cells were fixed with 4% paraformaldehyde and then stained with specific antibodies for 1 h at 4 °C. For intracellular molecule, the cells were pre-treated with 1 μg/mL ionomycin (MedChemExpress, 56092-81-0) and 50 ng/mL PMA (MedChemExpress, HY-18739) for 5 h in the presence of Brefeldin A (BioLegend, 420601) for the

Song *et al. Journal of Translational Medicine*   (2024) 22:1125

Page 4 of 17

last 4 h. The antibodies used for flow cytometry analysis were shown in Supplementary Table 2. FACSCelesta (BD Biosciences, USA) was used to detect the expression of molecules. The data were analyzed using the FlowJo software (Treestar Inc., Ashland, OR, USA).

The co-culture of T cells and macrophages

The splenic $CD8^+T$ cells of mice were sorted using a $CD8^+T$ cell sorting kit (Biolegend, 480008), and then activated with anti-CD3 (Biolegend, 100340) and anti-CD28 (Biolegend, 102116) antibodies. After CFSE staining for 15 min at 37 °C, these $CD8^+T$ cells were co-cultured with RAW264.7 cells pretreated with Napabucasin PLGA NPs at a ratio of 4:1 for 72 h. The proliferation and activation of $CD8^+T$ cells were detected by FACS Calibur (BD Biosciences, USA).

ECAR and OCR analysis

The RAW264.7 cells pre-treated with the supernatant of Hepa1-6 cells or not were inoculated in a Seahorse XFe24 Cell Culture Microplates (Agilent, Palo Alto, CA, USA). When cells were adhered, Napabucasin-PLGA NPs was added for 24 h. The medium was changed to Seahorse XF Base Medium and incubated in a non-CO_2 incubator for 1 h at 37 °C prior to the start of the assay. The assay was performed with the Seahorse XF Glycolysis Stress Test Kit (103020-100; Agilent) and Seahorse XF Cell Mito Stress Test Kit (103015-100; Agilent) according to the manufacturer's instructions, respectively. The data were collected and analyzed using XFe24 wave software (Agilent).

Statistical analysis

GraphPad Software Prism 8.0 (San Diego, CA, USA) was used for statistical analysis. Differences between two groups were tested for significance using the student t-test. All data are presented as mean ± standard error of the mean (mean ± SEM). Statistical comparisons between three or more groups were performed using one-way analysis of variance (ANOVA), followed by Tukey's multiple comparison test. Statistically significant differences were set at $*p < 0.05, **p < 0.01, ***p < 0.001$.

Results

The characterizations of Napabucasin-PLGA NPs

Napabucasin, as a novel STAT3 inhibitor, has shown excellent anti-tumor effects at both early and advanced stages of liver cancer in mouse models, and suppressive effects on the stem cell characteristics of HCC cells [10]. In order to improve its bioavailability and reduce toxicity, Napabucasin-PLGA NPs was prepared by solvent evaporation method. We observed that Napabucasin-PLGA NPs had the significant Tyndall effect (Fig. 1A).

The hydrodynamic size and polydispersity index (PDI) were evaluated by DLS, and the results showed that the hydrodynamic size of Napabucasin-PLGA NPs was about 300 nm and good dispersibility (Fig. 1B). The TEM detection displayed the morphology of the Napabucasin-PLGA NPs was spherical (Fig. 1C). The UV–vis spectrophotometry analysis showed that the encapsulation efficiency (EE%) of Napabucasin-PLGA NPs at a PLGA: Napabucasin ratio of 7.5:1 was over 90%, while the drug loading (DL%) was 11.18% (Figure S1). In addition, the release of Napabucasin-PLAG NPs under acidic condition (pH 5.0) was higher than that under physiological condition (pH 7.4), and the cumulative release amount of Napabucasin reached nearly to be 80% at 48 h (Fig. 1D), which shows slight pH responsive release characteristics of this NPs.

Napabucasin-PLGA NPs inhibited the viability of HCC cells

In order to verify whether Napabucasin-PLGA NPs could effectively exert anti-HCC effects like Napabucasin, we firstly plotted the dose–response curves of Napabucasin and Napabucasin-PLGA NPs in human HCC cell lines Huh7, Hepa3B and murine HCC cell line Hepa1-6 (Fig. 2A, B). The results showed that the IC50 value of Napabucasin-PLGA NPs was slightly increased compared with Napabucasin, but Napabucasin-PLGA NPs still exhibit effective anti-HCC effects. According to the IC50 value, Huh7, Hep3B and Hepa1-6 cells were treated with different concentrations of Napabucasin-PLGA NPs and Napabucasin in vitro. Similar to that of Napabucasin, we observed Napabucasin-PLGA NPs could inhibit HCC cell proliferation (Fig. 2C, D) and induce HCC cell apoptosis (Fig. 2E, F) in a dose- and time-dependent manner. These results suggested that Napabucasin-PLGA NPs had potential anti-HCC activity.

Napabucasin-PLGA NPs suppressed cancer-stemness of HCC cells in vitro

STAT3 is over-activated in a variety of tumors and is confirmed as an important pathway for tumor stemness [21]. Previously, we demonstrated Napacubucasin could inhibit the stemness of HCC cells in vitro [10]. Similarly, Napabucasin-PLGA NPs decreased the levels of p-STAT-3^{Try705} significantly in Huh7 cells (Fig. 3A), accompanied with the downregulation of tumor stemness-related molecules in HCC cells, including NANOG, SOX2, OCT4, and KIF4 (Fig. 3B). Next, we performed cell colony assay and sphere formation assay to evaluate the proliferation ability and stemness characteristics of HCC cells in vitro. Similar to the effect of Napabucasin, Napabucasin-PLGA NPs significantly reduced the colony formation of HCC cells (Fig. 3C) and the number of multicellular spheroids derived from Huh7 and Hepa1-6 cells (Fig. 3D). These results indicated that Napabucasin-PLGA NPs could
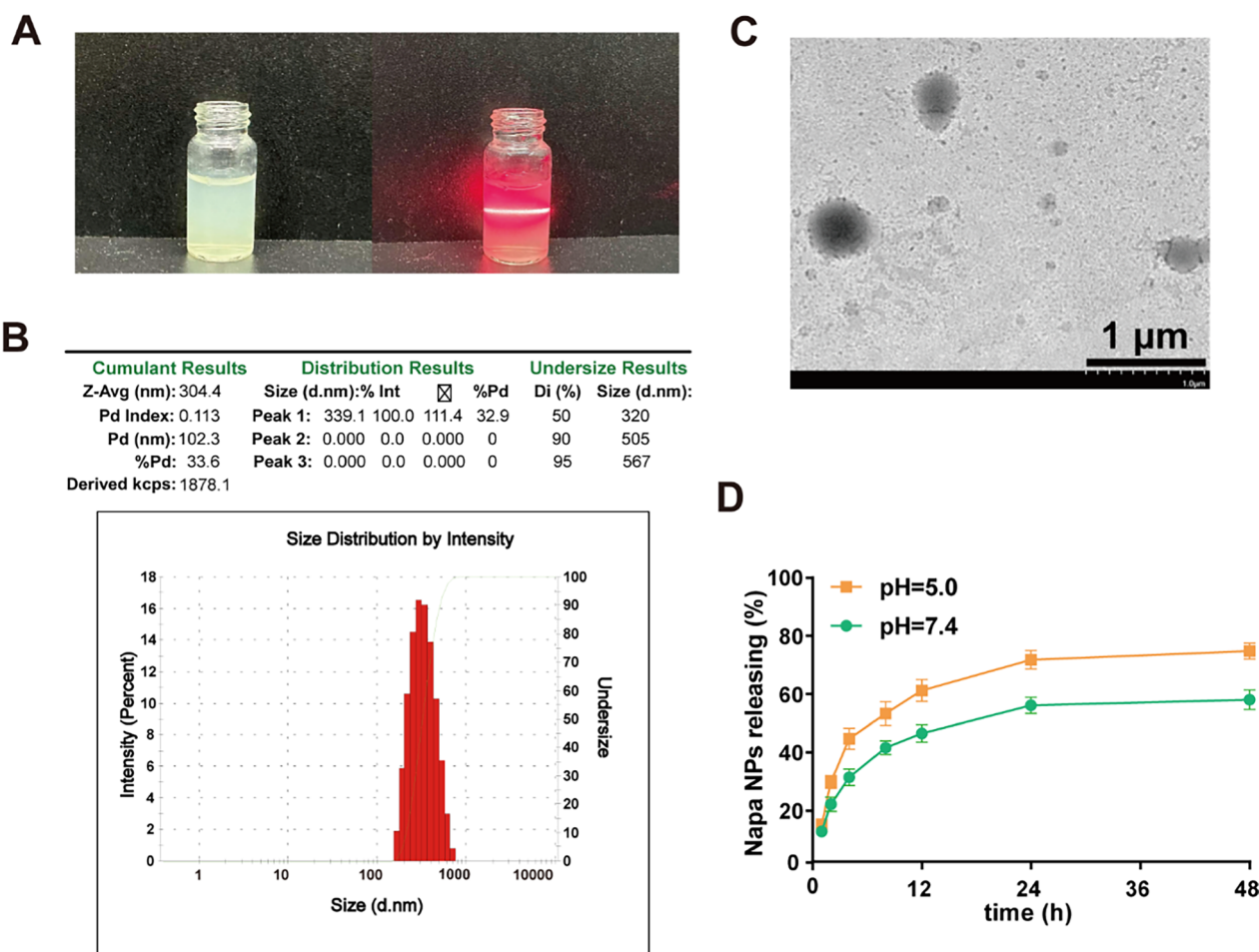
Fig. 1 Physicochemical properties of Napabucasin-PLGA NPs. **A** Tyndall effect was detected by laser irradiation. **B** The hydrodynamic size of Napabucasin-PLGA NPs was determined by dynamic light scatterer. **C** The TEM image of Napabucasin-PLGA NPs. **D** Release behavior curves of the Napabucasin-PLGA NPs in PBS under pH 5.0 and pH 7.4 conditions. Images are representatives of at least three independent experiments

suppress the stemness characteristics of HCC cells by disturbing STAT3 phosphorylation.

Napabucasin-PLGA NPs restrained HCC growth in mice with alleviative damage

Subsequently, we verified the therapeutic effects of Napabucasin-PLGA NPs in a subcutaneous homograft mouse model. On day 7 post of Hepa1-6 cell inoculation, these mice were treated intraperitoneally with Napabucasin or Napabucasin-PLGA NPs twice a day for total 8

times (Fig. 4A). Compared with untreated mice (PBS), Napabucasin-PLGA NPs displayed similar anti-HCC effects to Napabucasin (Fig. 4B–D). Notably, we observed the body weight of tumor-bearing mice was decreased by high-dose of Napabucasin (20 mg/kg) significantly (Fig. 4E), accompanied with severe damage in heart, liver, kidney, spleen and lung tissues, such as the enlargement of intercellular spaces in the kidney and a large number of vacuoles in the liver tissue (Fig. 4F). However, no significant tissue damage was observed in neither low- nor

(See figure on next page.)
Fig. 2 Napabucasin-PLGA NPs inhibit the viability of HCC cells in vitro. **A**, **B** Viability of HCC cells treated with different concentrations of Napabucasin (**A**) and Napabucasin-PLGA NPs (**B**) for 48 h. **C**, **D** Viability of HCC cells treated with Napabucasin (**C**) and Napabucasin-PLGA NPs (**D**) for 24 h, 48 h and 72 h. **E**, **F** After treated with Napabucasin or Napabucasin-PLGA NPs for 12 h, the apoptosis rate of Huh7 (**E**) and Hepa1-6 (**F**) cells was detected by Annexin V-PI using Flow cytometry. Napa, Napabucasin; Napa NPs, Napabucasin-PLGA NPs. Data are shown as mean ± SD from three independent experiments. Compared with 0 μM, one-way ANOVA with Tukey test. *$p < 0.05$, **$p < 0.01$, ***$p < 0.001$, ****$p < 0.0001$. ns, no significance
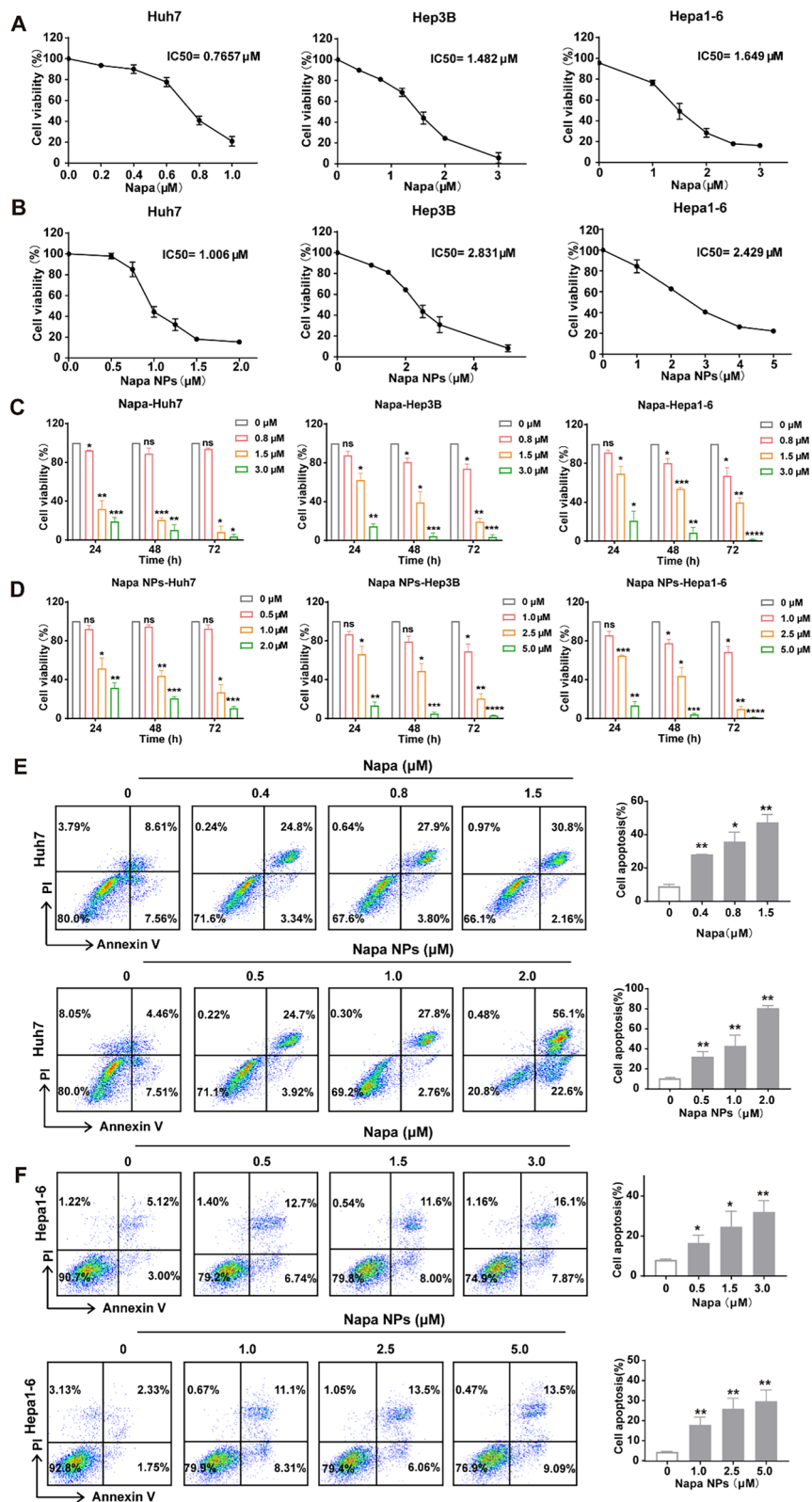
Fig. 2 (See legend on previous page.)

Song *et al. Journal of Translational Medicine*   (2024) 22:1125
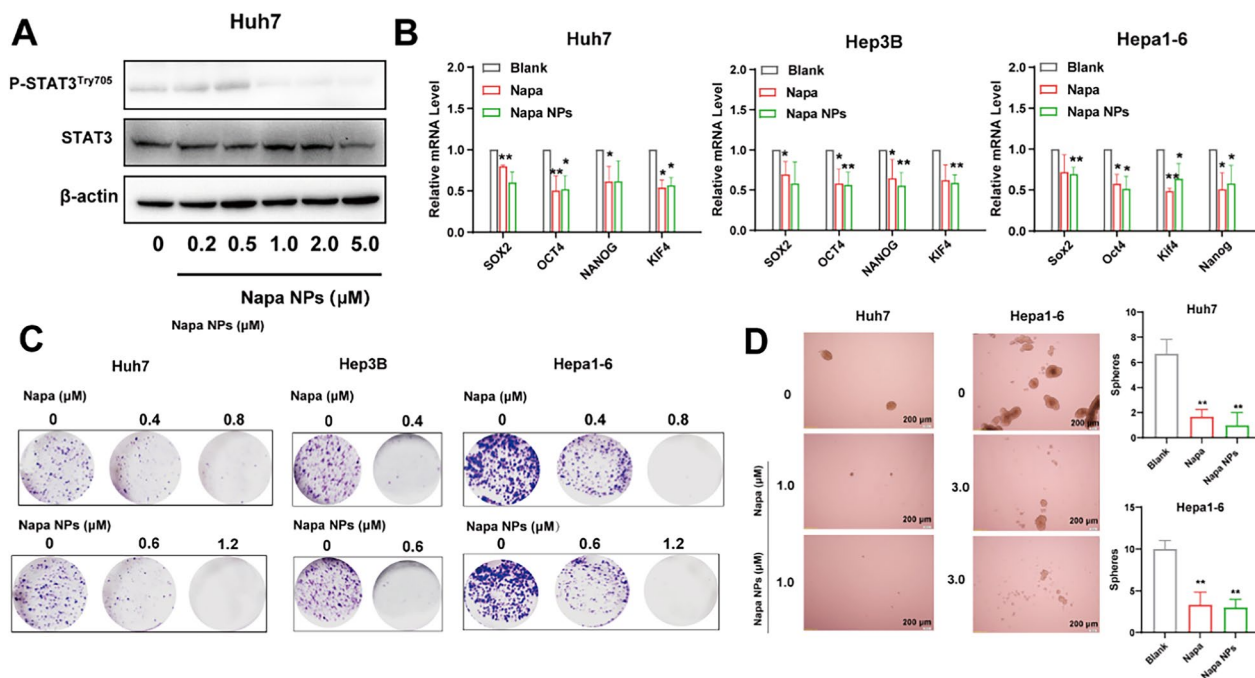
Page 7 of 17

Fig. 3 Napabucasin-PLGA NPs downregulate p-STAT3^Try705 levels and stemness characteristics of HCC cells. **A** Immunoblot showed STAT3 and p-STAT3^Try705 levels in Huh7 cells treated with different concentrations of Napabucasin-PLGA NPs. **B** The mRNA levels of stemness markers in HCC cells treated with Napabucasin (1 μM) or Napabucasin-PLGA NPs (1 μM) for 12 h. **C** HCC cells were treated with different concentrations of Napabucasin or Napabucasin-PLGA NPs, and the colony formation was detected on day 15. **D** HCC cells were treated with Napabucasin or Napabucasin-PLGA NPs, and the sphericity was detected on day 10. Napa, Napabucasin; Napa NPs, Napabucasin-PLGA NPs. Data are shown as mean ± SD from three independent experiments. Compared with 0 μM, one-way ANOVA with Tukey test. *$p < 0.05$, **$p < 0.01$

high-dose of Napabucasin-PLGA NPs treated mice (Fig. 4G). These data suggested that Napabucasin-PLGA NPs exerted favorable anti-HCC effects and reduced the risk of toxic side effects of Napabucasin.

Napabucasin-PLGA NPs improved tumor immune microenvironment

The progression of tumors is closely related to the immune microenvironment. Along with tumor development, the important anti-tumor lymphocytes such as effector CD8^+T cells and NK cells are functionally exhausted in the tumor microenvironment (TME) with increased levels of immune checkpoints such as PD-1, TIGIT, TIM3 and LAG3. Then, we explored the effects of Napabucasin-PLGA NPs on the immune responses in the subcutaneous homograft mouse model of Hepa1-6 cells (Fig. 5A). The results showed both empty nanoparticles (Empty NPs) and Napabucasin-PLGA NPs could increase the proportion of CD8^+T cells in tumor tissues compared to the untreated mice (PBS) (Fig. 5B), but Napabucasin-PLGA NPs treatment promoted the production of IFN-γ and TNF-α in CD8^+T cells (Fig. 5C), and down-regulated the checkpoint molecule TIGIT (Fig. 5D). In addition, Napabucasin-PLGA NPs augmented the infiltration of NK cells (Fig. 5E), accompanied with the increased

production of TNF-α (Fig. 5F) and decreased expression of TIGIT and TIM3 (Fig. 5G). The infiltration of CD4^+T cells was also enhanced by Napabucasin-PLGA NPs with elevated levels of TNF-α (Fig. 5H).

Tumor associated macrophages (TAMs) are one of the most abundant immune components in tumor microenvironment, and the M2 polarization of TAMs is closely related to the development of tumors [22]. We observed that Napabucasin-PLGA NPs treatment increased the infiltration of macrophages (Fig. 5I) compared with untreated or Empty NPs treated mice, accompanied with the downregulation of CD206 (Fig. 5J), a marker of M2 macrophages. Meanwhile, the levels of M1 markers iNOS, CD86 and MHC II in macrophages were up-regulated (Fig. 5K) by Napabucasin-PLGA NPs. Moreover, the expression of PD-L1 on tumor infiltrated macrophages from mice treated with Napabucasin-PLGA NPs was lower than that from other groups (Fig. 5L). These findings indicated that Napabucasin-PLGA NPs could improve the tumor immune microenvironment of HCC.

Napabucasin-PLGA NPs promoted the M1 polarization of TAMs

To understand whether Napabucasin-PLGA NPs directly affect the polarization and function of HCC-induced
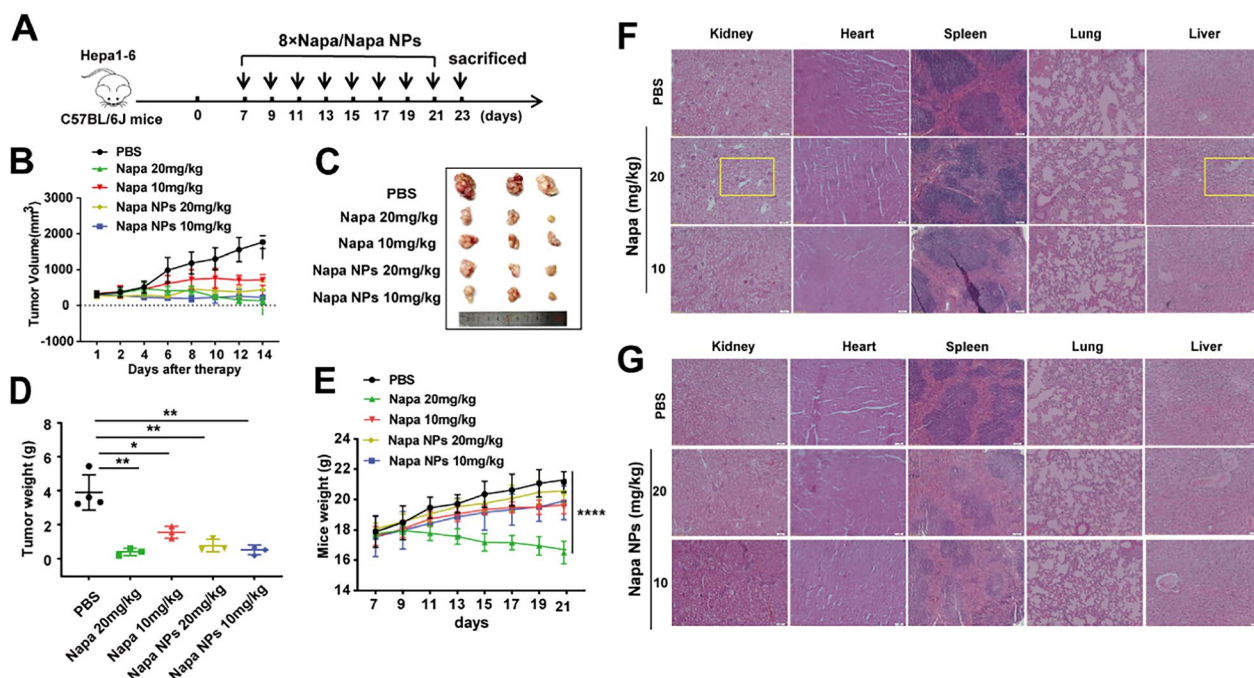
Song *et al. Journal of Translational Medicine*   (2024) 22:1125

Page 8 of 17

Fig. 4 Napabucasin-PLGA NPs inhibit HCC growth in vivo. **A** Schematic diagram of the treatment regimen for the subcutaneous homograft mouse model. **B** The growth curves of tumors in each group; n = 3/4. **C** The image of subcutaneous tumors from each group. **D** The average tumor weight of each group. **E** Body weight curves of tumor-bearing mice. **F**, **G** HE staining was performed to evaluate the damage of heart, liver, spleen, lung, and kidney from tumor-bearing mice treated with Napabucasin (**F**) and Napabucasin-PLGA NPs (**G**). Napa, Napabucasin; Napa NPs, Napabucasin-PLGA NPs. Data are shown as mean ± SD, and compared with PBS, one-way ANOVA with Tukey test. *$p < 0.05$, **$p < 0.01$, ****$p < 0.0001$

(See figure on next page.)

Fig. 5 Napabucasin-PLGA NPs improve the tumor immune microenvironment. The phenotype and activation of tumor-infiltrating immune cells from HCC-bearing mice were assessed by flow cytometry. **A** The gating strategy for tumor-infiltrating immune cells. The percentages of CD8+T cells (**B**), IFN-γ+-, TNF-α+- (**C**) and TIGIT+CD8+T cells (**D**). The percentages of NK cells (**E**), IFN-γ+ NK cells (**F**), TIGIT+- and TIM3+ NK cells (**G**). The percentages of tumor-infiltrated CD4+T and TNF-α+CD4+T cells (**H**). The frequency of CD11b+F4/80+ macrophages (**I**), CD206+ macrophages (**J**), iNOS+-, MHC II+-, CD86+ macrophages (**K**) and PD-L1+macrophages (**L**). n = 6. Napa NPs, Napabucasin-PLGA NPs. Data are shown as mean ± SD, one-way ANOVA with Tukey test. *$p < 0.05$, **$p < 0.01$, ***$p < 0.001$. ns, no significance

TAMs, RAW264.7 cells (a murine macrophage cell line) were treated with the culture supernatant from Hepa1-6 cells (TCM) to induce HCC-TAMs with M2-like phenotype (Fig. 6A, B). Furthermore, the culture supernatant (CM) from these HCC-TAMs (Fig. 6C) could promote the proliferation (Fig. 6D) and migration (Fig. 6E) of Hepa1-6 cells, indicating HCC-induced TAMs exhibited tumor-promoting function of M2-like TAMs.

STAT3 is over-activated in TAMs and promotes M2 macrophage polarization [23]. Compared with RAW264.7 cells cultured in medium (Naive), we found p-STAT3^{Try705} levels were significantly increased in HCC-TAMs (Untr), which could be significantly decreased by the treatments of Napabucasin-PLGA NPs and Napabucasin (Fig. 6F). Furthermore,

Napabucasin-PLGA NPs showed more potent inhibitory effect on the proliferation ability of HCC-TAMs than Napabucasin (Fig. 6G). Significantly, compared to Empty-NPs, Napabucasin-PLGA NPs reduced the mRNA levels of M2 markers such as CD206, IL-10 and TGF-β in HCC-TAMs, and increased M1 markers iNOS and IL-12 mRNA levels (Fig. 6H). Consistently, the ratio of CD206/iNOS in HCC-TAMs was obviously decreased by the treatment of Napabucasin-PLGA NPs, accompanied with the increase of IL-12 (Fig. 6I). In addition, the culture supernatant from Napabucasin-PLGA NPs-treated HCC-TAMs (Fig. 6J) could inhibit the proliferation (Fig. 6K) and migration ability (Fig. 6L) of Hepa1-6 cells. These results demonstrated that Napabucasin-PLGA NPs could directly influence the phenotype and convert tumor-promoting HCC-TAMs to anti-tumor HCC-TAMs.
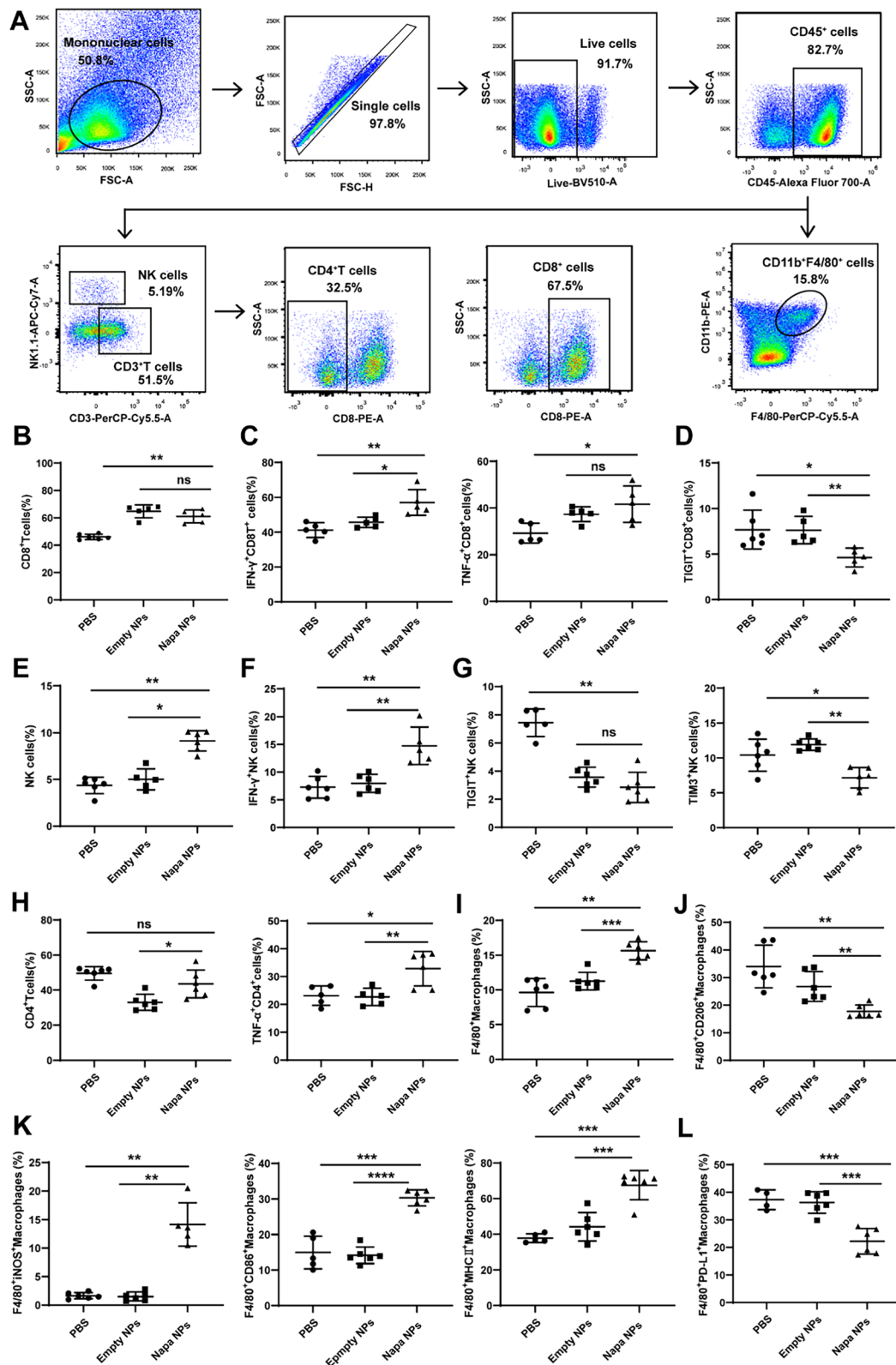
Song *et al. Journal of Translational Medicine*   (2024) 22:1125

Page 9 of 17

Fig. 5 (See legend on previous page.)

Song *et al. Journal of Translational Medicine*   (2024) 22:1125
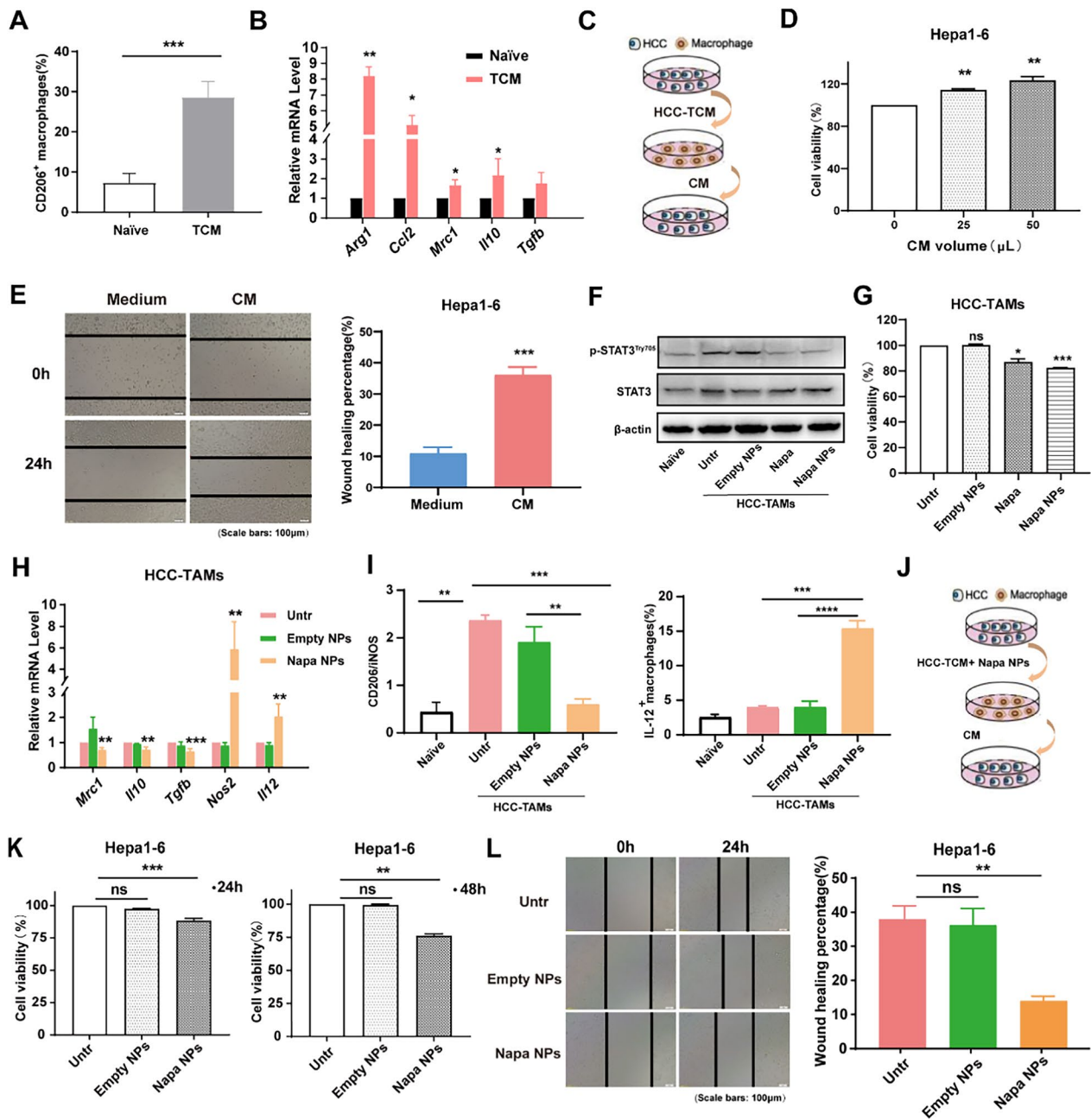
Page 10 of 17

Fig. 6 Napabucasin-PLGA NPs convert M2 type tumor-promoting HCC-TAMs to M1 type anti-tumor HCC-TAM. **A**, **B** RAW264.7 cells were incubated with TCM from Hepa1-6 cells for 48 h to induce HCC-TAMs. The expression levels of CD206 on RAW264.7 cells were detected by flow cytometry (**A**). Transcription levels of markers for M2 macrophages were determined by RT-qPCR (**B**). **C**, **D** The supernatant of HCC-TAMs (CM) was collected to incubate Hepa1-6 cells (**C**). The cell viability of Hepa1-6 cells treated with indicated volumes of CM for 24 h was detected by CCK-8 assay (**D**). **E** Hepa1-6 cells were scratched with a plastic pipette tip and incubated with culture medium (Medium) or CM for 24 h. **F** Immunoblot analysis for STAT3 and p-STAT3^{Try705} levels in HCC-TAMs treated with Napabucasin (3 µM), Napabucasin-PLGA NPs (3 µM) or Empty NPs. **G** Viability of HCC-TAMs incubated with Napabucasin (3 µM), Napabucasin-PLGA NPs (3 µM) for 24 h. **H** The mRNA levels of M2 and M1 markers in HCC-TAMs treated with Napabucasin-PLGA NPs (3 µM) or Empty NPs were determined by RT-qPCR. **I** The ratio of CD206/iNOS and IL-l2 level in HCC-TAMs treated with Napabucasin-PLGA NPs (3 µM) or Empty NPs for 24 h were measured by flow cytometry. **J**–**L** HCC-TAMs were treated with Napabucasin-PLGA NPs (3 µM) and Empty NPs for 24 h. Then, these HCC-TAMs were cultured with fresh medium for 24 h, and the supernatants (CM) were collected to treat Hepa1-6 cells (**J**). The viability of Hepa1-6 cells incubated with CM for 24 h and 48 h was tested by CCK8 assay (**K**). The migration ability of Hepa1-6 cells was detected by cell scratches (**L**). Naive, RAW264.7 cells incubated in culture medium; Untr, untreated HCC-TAMs; Napa, Napabucasin; Napa NPs, Napabucasin-PLGA NPs. Data are shown as mean ± SD from three independent experiments. *$p < 0.05$, **$p < 0.01$, ***$p < 0.001$. ns, no significance

Song *et al. Journal of Translational Medicine*   (2024) 22:1125

Page 11 of 17

Napabucasin-PLGA NPs suppressed FAO in HCC-TAMs

Macrophages exhibit extremely strong metabolic plasticity. In the TME, the metabolic pathways in macrophages were changed by metabolic reprogramming, obtaining sufficient energy and metabolic intermediates to meet the demands for biosynthesis, proliferation, differentiation and functions [24]. M2 macrophages predominantly use oxidative phosphorylation (OXPHOS) to generate ATP for the energy. By Seahorse energy metabolism assay, we found both ECAR (Extracellular acidification rate) and OCR (Oxygen consumption rate) levels were significantly increased in HCC-TAMs compared to control macrophages (Naive), which could be markedly suppressed by Napabucasin-PLGA NPs. Especially, the reduction of OCR level was greater than ECAR (Fig. 7A, B). Commonly, lipid accumulation is increased in TAMs of tumor tissues. Free long-chain fatty acids provide raw materials and metabolic intermediates for OXPHOS through fatty acid β-oxidation (FAO), and the enhanced FAO process is also one of the metabolic characteristics of TAMs [25]. Through GEPIA2 database analysis, we found that STAT3 in HCC was positively correlated with many enzymes involved in FAO process such as CPT1A, CPT2, ACADM, HADHA and ACACA (Fig. 7C), indicating the activation of STAT3 might contribute to the FAO process.

BODIPY staining showed increased lipid accumulation in HCC-TAMs (Fig. 7D). Unexpectedly, Napabucasin-PLGA NPs further enhanced lipid accumulation in HCC-TAMs. To understand whether Napabucasin-PLGA NPs augment lipid uptake, we detected the mRNA levels of fatty acid transporters CD36, CD69 and MARCO in HCC-TAMs. The results showed Napabucasin-PLGA NPs did not influence the mRNA levels of these molecules (Fig. 7E). Next, we examined the mRNA levels of FAO-related molecules in HCC-TAMs. We found the mRNA levels, including CPT1A, CPT1B, ACADM, ECHS1 and ACACA, were elevated in HCC-TAMs (Fig. 7F), which could be obviously decreased by Napabucasin-PLGA NPs (Fig. 7G). Therefore, Napabucasin-PLGA NPs reduced lipid consumption by inhibiting FAO process, resulting in the enhanced lipid accumulation in HCC-TAMs.

CPT1 is responsible for transporting activated fatty acids to mitochondria and is the rate-limiting enzyme in the FAO process. To confirm the role of FAO process on M2-polariztion of HCC-TAMs, CPT1A over-expression vectors were transfected into HCC-TAMs. We found the overexpression of CPT1A could resist the inhibitory effect of Napabucasin-PLGA NPs on FAO-related molecules (Fig. 7H) and M2-type polarization of HCC-TAMs (Fig. 7I, J). Collectively, these findings indicated Napabucasin-PLGA NPs disturbed OXPHOS via inhibiting FAO process, leading to the suppression of M2 polarization of HCC-TAMs.

Napabucasin-PLGA NPs augmented T cell-mediated anti-HCC effects

To understand whether T cells involved in Napabucasin-PLGA NPs induced anti-HCC effects, CD8$^+$T cells were isolated from the spleen of mice by magnetic bead and stimulated with anti-CD3/CD28 antibodies in vitro, and then co-incubated with HCC-TAMs pre-treated with Napabucasin-PLGA NPs or not for 72 h. Compared with T cells alone, HCC-TAMs could inhibit the proliferation of CD8$^+$T cells, which could be significantly relieved by pre-treatment of Napabucasin-PLGA NPs (Fig. 8A). Moreover, HCC-TAMs pre-treated with Napabucasin-PLGA NPs increased the production of IFN-γ, Perforin and Granzyme B by CD8$^+$T cells, accompanied with the downregulation of immune checkpoint molecule PD-1 (Fig. 8B). However, when CD8$^+$T cells were co-cultured with HCC-TAMs pre-treated with Napabucasin-PLGA NPs or not using Transwell method, no significant change was shown in the proliferation of CD8$^+$T cells (Fig. 8C), suggesting HCC-TAMs disturbing CD8$^+$T cells through cell-to-cell interaction. Furthermore, we verified the anti-tumor effects of T cells in Napabucasin-PLGA NPs treatment by eliminating CD4$^+$T or CD8$^+$T cells in the Hepa1-6 subcutaneous homograft mouse model (Fig. 8D). Compared with untreated (PBS) or Empty NPs

(See figure on next page.)

Fig. 7 Napabucasin-PLGA NPs inhibit FAO in HCC-TAMs. **A** The levels of ECAR, glycolysis, glycolytic reserve, glycolytic capacity of HCC-TAMs treated as indicated for 24 h. **B** The levels of OCR, basal respiration, ATP production, spare respiratory capacity of HCC-TAMs treated as indicated for 24 h. **C** The analysis of correlation between FAO-related molecules and STAT3 in HCC through GEPIA 2 database. **D** The lipid levels of RAW264.7 cells cultured in medium (Naive) and HCC-TAMs treated as indicated were detected by flow cytometry. **E** The mRNA levels of CD36, CD69 and Macro in HCC-TAMs treated with Napabucasin-PLGA NPs or not were determined by RT-qPCR. **F** The mRNA levels of FAO-related genes in RAW264.7 cells cultured in medium (Naive) and HCC-TAMs were determined by RT-qPCR. **G** The mRNA levels of FAO-related genes in HCC-TAMs treated with Napabucasin-PLGA NPs or Empty NPs for 24 h were determined by RT-qPCR. **H, I** The mRNA levels of FAO-related (**H**) and M2 markers (**I**) in HCC-TAMs treated as indicated for 24 h were determined by RT-qPCR. **J** The levels of CD206, iNOS in HCC-TAMs treated as indicated for 24 h were measured by flow cytometry. Naive, RAW264.7 cells incubated in culture medium; Untr, untreated HCC-TAMs; Napa NPs, Napabucasin-PLGA NPs (3 μM); ov-CPTIA, HCC-TAMs over-express CPT1A. Data are shown as mean ± SD from three independent experiments. *$p < 0.05$, **$p < 0.01$, ***$p < 0.001$. ns, no significance
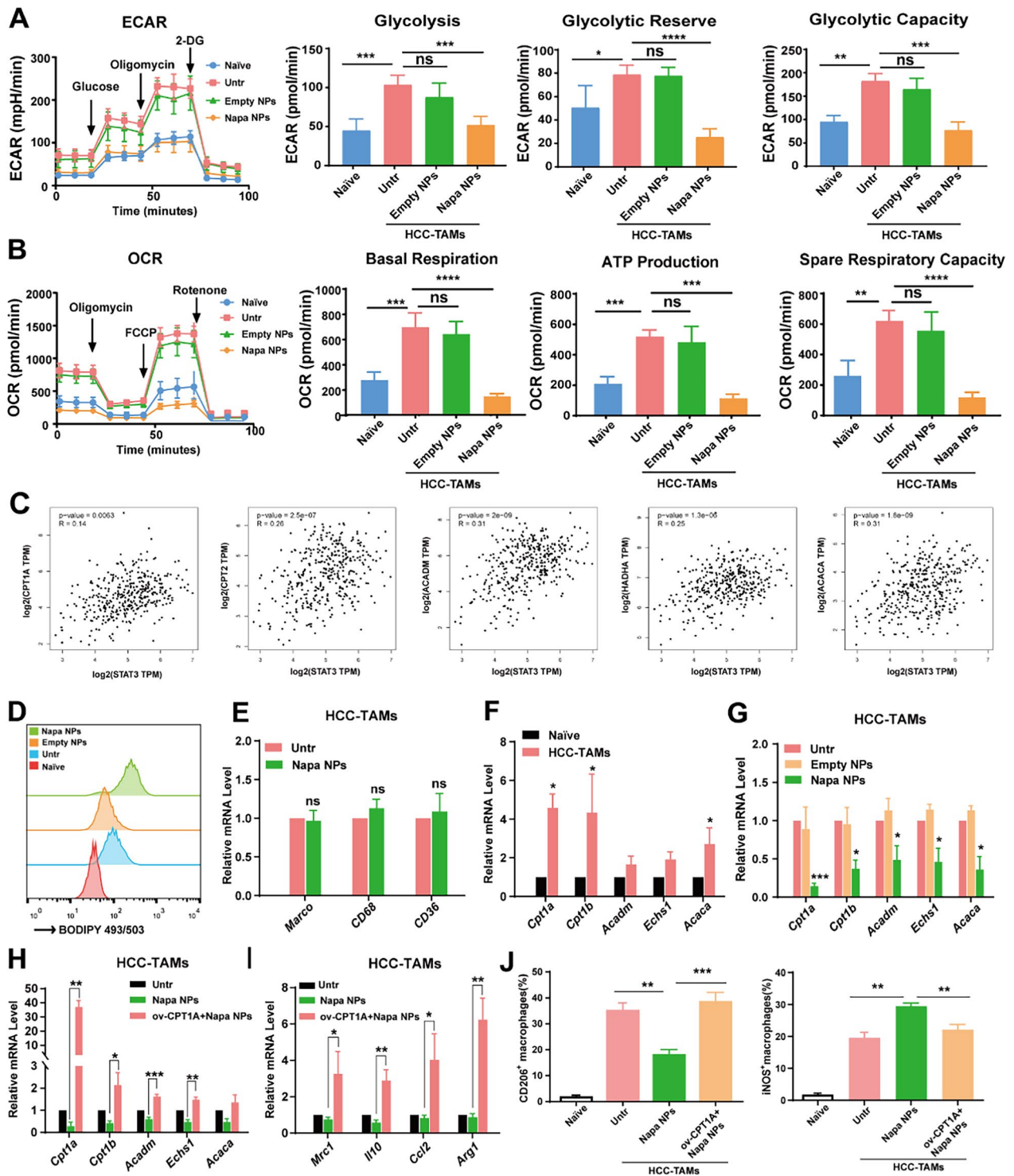
Fig. 7 (See legend on previous page.)

treated mice, the tumor growth was obviously suppressed in mice treated with Napabucasin-PLGA NPs, which was significantly weakened by the depletion of CD8^{+}T and CD4^{+}T cells, especially CD8^{+}T cells (Fig. 8E–G). These

Song *et al. Journal of Translational Medicine*   (2024) 22:1125
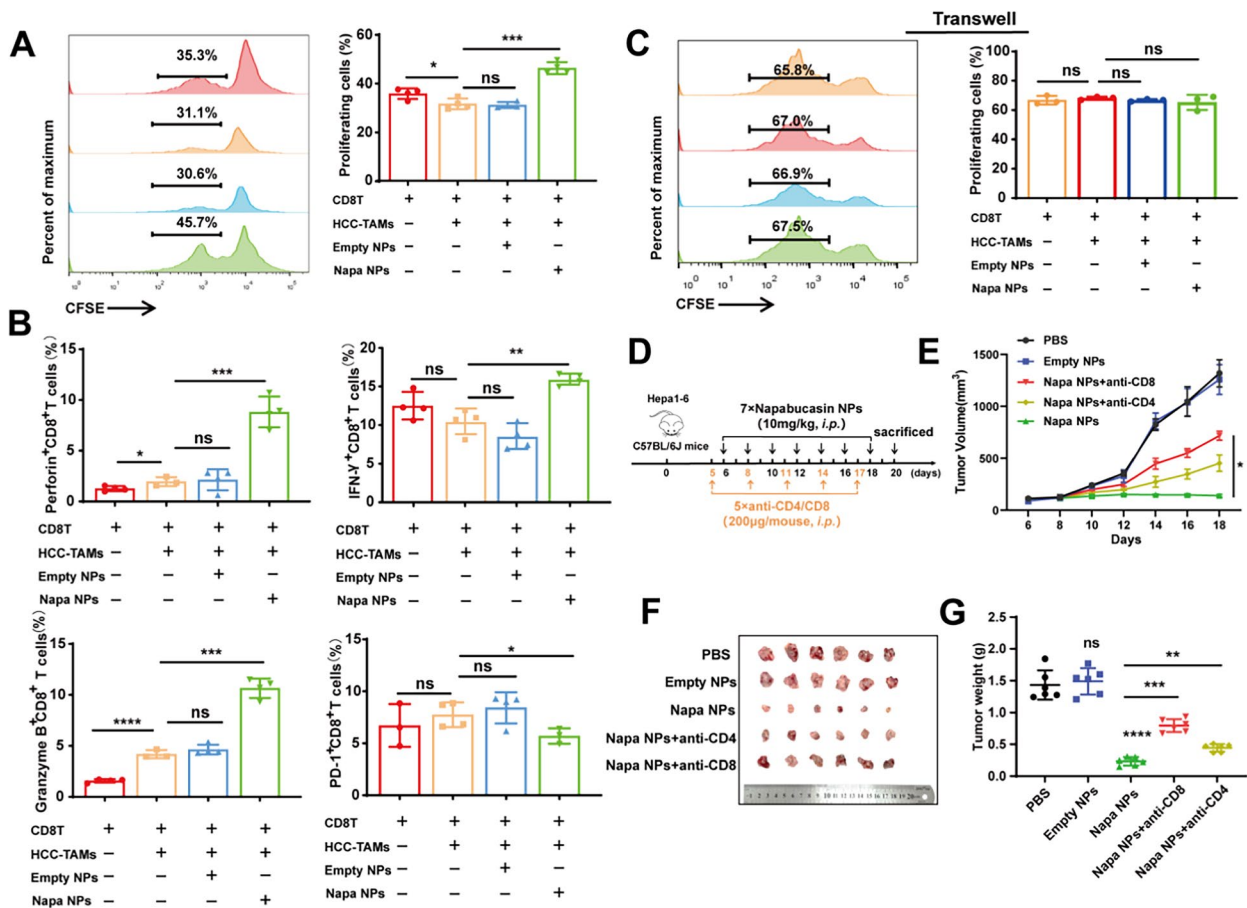
Page 13 of 17

Fig. 8 Napabucasin-PLGA NPs enhance T cell-mediated anti-HCC immune responses. **A**–**C** CFSE-labelled CD8+T cells were activated with anti-CD3 and anti-CD28 antibodies, and then co-cultured with HCC-TAMs pre-treated by Napabucasin-PLGA NPs (3 μM) or Empty NPs in a ratio 4:1 for 72 h. The proliferation of (**A**) and the production of IFN-γ, Perforin, Granzyme B and PD-1 (**B**) in these CD8+T cells were measured by flow cytometry. **C** CFSE-labelled T cells activated with anti-CD3 and anti-CD28 antibodies, and then co-cultured with HCC-TAMs treated as above in Transwell. The proliferation of CD8+T cells was analyzed by flow cytometry. **D** Experimental scheme for the subcutaneous homograft mouse model in C57BL/6J mice. **E** The tumor growth curves. **F** Image of the subcutaneous tumors from each group. **G** The average tumor weight of each group. n = 6. Napa NPs, Napabucasin-PLGA NPs. Data are shown as mean ± SD, one-way ANOVA with Tukey test. *$p < 0.05$, **$p < 0.01$, ***$p < 0.001$, ****$p < 0.0001$. ns, no significance

results suggest T cells are important effector cells in anti-HCC treatment of Napabucasin-PLGA NPs.

Discussion

The occurrence of HCC is a complex multi-step process, which is regulated by many factors such as genetics and environment, and associated with the abnormal activation of various carcinogenic signaling pathways [26]. Studies have shown that overexpression and constitutive activation of STAT3 are closely related to the pathogenesis of HCC [4, 27], and liver cancer tissues with high activated STAT3 levels are more aggressive [28]. Although STAT3 knockdown is embryonic lethal, STAT3 inhibitor or local knockdown of STAT3 does not influence the survival of differentiated cells [29], so STAT3 signaling

pathway has become a potential target for pharmacological intervention in cancer therapy [30]. Napabucasin is the only STAT3 inhibitor that has entered phase III clinical trials. It can interfere STAT3 phosphorylation and down-regulate the expression of tumor stemness-related genes such as *β-catenin*, *NANOG* and *SOX2*, inhibiting the proliferation and survival of a variety of cancer cells and preventing cancer recurrence and metastasis [21, 31]. In order to improve the bioavailability and reduce the dosage and side effects of Napabucasin in vivo, we prepared Napabucasin-PLGA NPs and evaluated it's anti-HCC efficiency. The hydrodynamic size of Napabucasin-PLGA NPs was about 300 nm with a good dispersibility and spherical morphology. Notably, Napabucasin-PLGA NPs showed slight pH responsive release characteristic,

Song *et al. Journal of Translational Medicine*   (2024) 22:1125

Page 14 of 17

which can increase the release of Napabucasin in the acidic environment of tumor tissue and decrease the cytotoxicity to normal tissues. The results proved that Napabucasin-PLGA NPs still exerted excellent anti-HCC effects, demonstrating nano-formulation did not influence the drug properties of Napabucasin. Significantly, low-dose of Napabucasin-PLGA NPs could obviously inhibit HCC growth in mice with no obvious effect on the body weight or vital organs of tumor-bearing mice. Therefore, PLGA NPs improved the bioavailability of Napabucasin, augmenting the anti-HCC efficiency and safety of Napabucasin. In addition to the direct inhibitory effects on the tumor biologic characteristics of HCC, we found Napabucasin-PLGA NPs also improved tumor microenvironment to enhance the anti-HCC immunity.

TME is a highly complex and heterogeneous ecosystem, which is composed of tumor-infiltrating immune cells, cancer-associated fibroblasts (CAFs), smooth muscle cells, endothelial cells and tumor cells [32, 33]. TME can promote cancer progression and mediate therapeutic resistance, especially for anti-tumor immunotherapy [34, 35]. More and more evidences show that STAT3 is over-activated not only in tumor cells, but also in immune cells such as TAMs in TME [36–38], significantly impacting on anti-tumor immunity by multiple mechanisms. TAMs are one of the most abundant immune cells in the TME and tend to be M2 phenotype, mediating the regression of inflammatory response and tissue repair. In addition, TAMs with high heterogeneity and plasticity are an important factor for the establishment of the premetastatic niche, priming the growth and metastasis of tumor [39]. Now, reprogramming TAMs polarization has become an important strategy for cancer therapy. TAMs play an important role in regulating the progression of HCC, and we observed that HCC supernatant could induce the constitutive activation of STAT3 and M2-type of TAMs. Interestingly, Napabucasin-PLGA NPs could directly inhibit STAT3 activation in HCC-TAMs in vitro, and promote the transformation of M2- into M1-type HCC-TAMs in vitro and in TME of tumor-bearing mice.

Increasing evidences show the activation of macrophages is closely related to metabolic reprogramming. The changes of metabolic patterns are crucial for macrophages to defend against host infection, clear pathogens and repair tissue damage [40]. Macrophages have extensive metabolic adaptability to respond to multiple stimuli in TME. Aerobic glycolysis and OXPHOS are two important metabolic pathways and are closely related to the polarization of macrophages. For M1 macrophages, TCA cycle and OXPHOS are generally impaired, while the glycolysis is the major metabolic mode [41]. Glycolysis facilitates the rapid production of ATP to maintain the phagocytosis of macrophages, and provides metabolic precursors for the pentose phosphate pathway. As a pluripotent transcription factor, STAT3 increases glycolysis by upregulating the key enzymes such as HIF-1α, GLUT1 and PKM2 in the process of glycolysis [42]. Recent studies show M2-type macrophages induced by IL-4 exhibited enhanced glycolysis levels [15]. And, our previous studies also proved that inhibiting glycolysis in TAMs can impede M2 polarization [43]. Here, we observed Napabucasin-PLGA NPs could decrease ECAR level of HCC-TAMs, indicating Napabucasin-PLGA NPs might suppress M2 polarization via disrupting STAT3-regulated glycolysis in HCC-TAMs. More significantly, we found Napabucasin-PLGA NPs exhibited stronger suppressive effect on OXPHOS than on glycolysis of HCC-TAMs. M2-type macrophages have the complete TCA cycle, and the oxygen consumption are increased significantly in activated macrophages, hence OXPHOS pathway and FAO process become the important energy supply ways [44]. FAO is the major way for long-chain fatty acids in mitochondrial metabolism, and an important way for cells to obtain energy. FAO process is complex and involves the activation, transfer and β-oxidation of fatty acids, and finally acetyl CoA is completely oxidized through the TCA cycle to CO_2 and H_2O, and release energy. In this study, Database analysis suggested that STAT3 was positively correlated with many enzymes in the process of FAO. And, we observed lipid accumulation was increased in HCC-TAMs, accompanied by a significant upregulation of metabolic enzymes related to FAO. Significantly, Napabucasin-PLGA NPs could inhibit OXPHOS process in HCC-TAMs by disturbing the FAO, reducing endogenous lipid consumption and OCR levels, which converted the M2-polarization of HCC-TAMs to M1-type polarization HCC-TAMs. Therefore, Napabucasin-PLGA NPs promoted the conversion of M2-type to M1-type HCC-TAMs via suppressing both glycolysis and OXPHOS processes.

In TME, TAMs continuously interact with tumor-infiltrated T cells. By secreting high levels of inhibitory cytokines such as IL-10 and TGF-β, M2-type TAMs up-regulate the expression of immune checkpoint molecules such as PD-1, TIGIT, TIM3 and LAG3 on the surface of T cells, but down-regulate the production of IFN-γ and IL-2 by T cells, inducing $CD8^+T$ cells exhaustion and damage of anti-tumor immunity. Targeted elimination of $CD163^+TAMs$ in tumor tissue can significantly enhance the infiltration of $CD8^+T$ cells and inhibit tumor growth [45]. In our study, we found HCC-TAMs disrupted $CD8^+T$ cells mainly through cell–cell interaction in vitro. And, Napabucasin-PLGA NPs could relieve the inhibitory effects of HCC-TAMs on $CD8^+T$ cells, promoting $CD8^+T$ cell proliferation and function. In tumor-bearing mice,

Song *et al. Journal of Translational Medicine*   (2024) 22:1125

Page 15 of 17

Napabucasin-PLGA NPs promoted the transformation of M2- into M1-type TAMs, accompanied with the up-regulation of MHC II and CD86 and the decrease of PD-L1. Simultaneously, Napabucasin-PLGA NPs augmented the production of IFN-γ and TNF-α in CD8⁺T cells and decreased the checkpoint molecule TIGIT. However, the depletion of CD8⁺T cells significantly impaired the therapeutic effects of Napabucasin-PLGA NPs. These results indicated that Napabucasin-PLGA NPs treatment could enhance the antigen presentation function of HCC-TAMs, reversing the exhaustion of CD8⁺T cells to play an important role in anti-tumor effects. In addition, the elimination of CD4⁺T cells also showed significant impact on the anti-tumor response triggered by Napabucasin-PLGA NPs. CD4⁺T cells can differentiate into different cell subtypes to assist the immune responses. For instance, Th17 cells can cooperate with CD8⁺T cells to kill tumor cells, and the immune balance between Th17 and Tregs is also crucial for maintaining immune homeostasis [46]. We noted that Napabucasin-PLGA NPs also promoted the infiltration and activation of NK cells in tumor tissues, indicating NK cells also participated in Napabucasin-PLGA NPs-triggered anti-HCC immune responses. Therefore, the interaction between TAMs and CD4⁺T or NK cells was also worth further exploration in the future.

In summary, as shown in Fig. 9, our study demonstrated that Napabucasin-PLGA NPs exhibited excellent anti-HCC effects and reduced the risk of toxic side effects of Napabucasin. On the one hand, Napabucasin-PLGA NPs directly disturbed the tumor biologic properties of HCC cells such as the viability and cancer-stemness. On the other hand, Napabucasin-PLGA NPs could inhibit STAT3 phosphorylation in HCC-TAMs, and induce the metabolic reprogramming in HCC-TAMs via disturbing FAO process, which suppressed M2-type polarization and enhanced the antigen presentation ability of HCC-TAMs, recovering T cell function and augmenting anti-tumor immune responses. Therefore, Napabucasin-PLGA NPs is a potential therapeutic candidate for HCC.
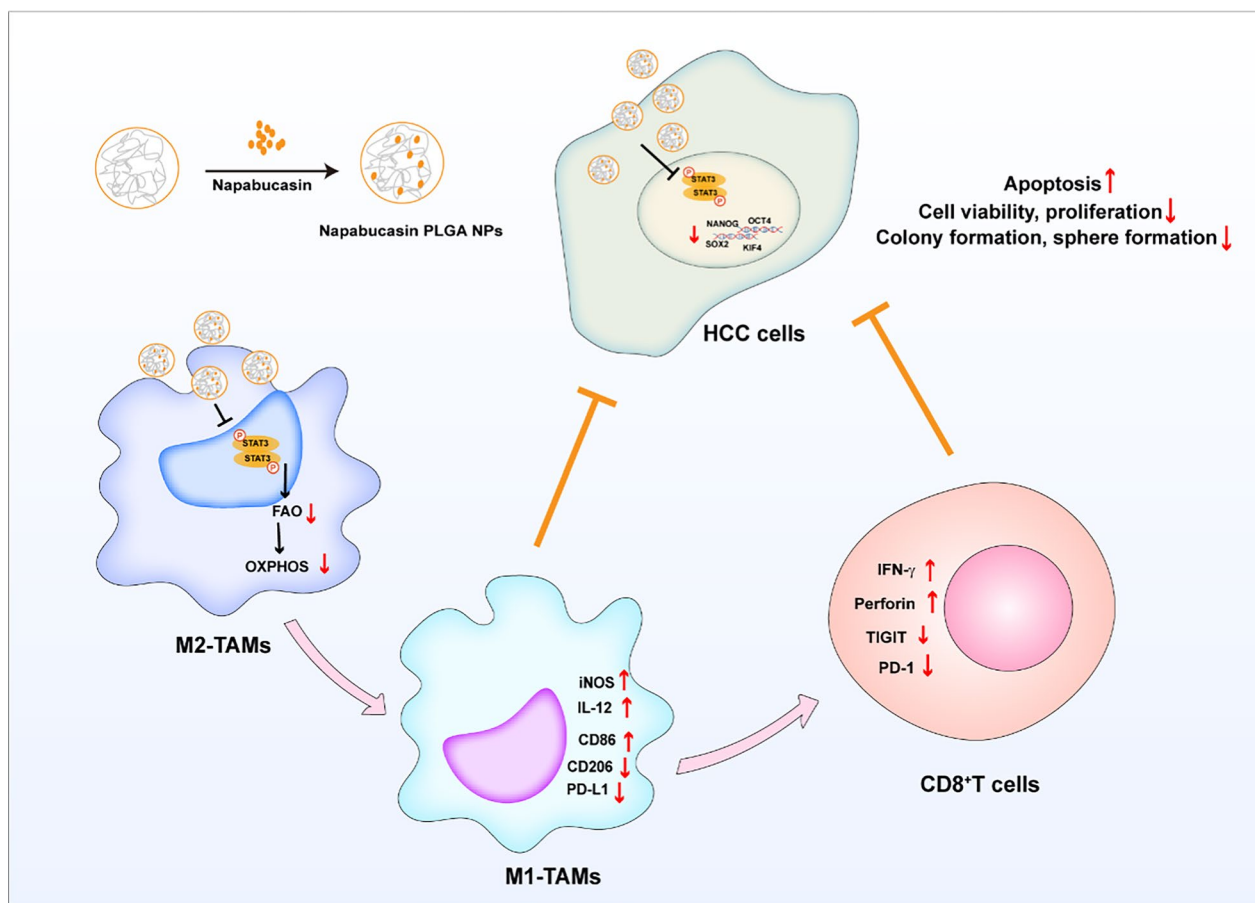

Fig. 9 Schematic diagram of the anti-HCC effects of Napabucasin-PLGA NPs. Napabucasin-PLGA NPs can downregulate the phosphorylation of STAT3 in HCC and inhibit the biological characteristics of tumor. Meanwhile, Napabucasin-PLGA NPs can reprogram HCC-TAMs through STAT3-FAO axis, thus improving the tumor microenvironment and enhancing CD8⁺ T cell anti-tumor function

Song *et al. Journal of Translational Medicine*   (2024) 22:1125

Page 16 of 17

Abbreviations

CAF	Cancer associated fibroblasts
CCL2	C-C motif chemokine 2
FAO	Fatty acid oxidation
GLUT1	Facilitative glucose transporter 1
HCC	Hepatocellular carcinoma
HE	Hematoxylin–eosin staining
IFN-γ	Interferon-γ
iNOS	Inducible nitric oxide synthase
NPs	Nano particles
OXPHOS	Oxidative phosphorylation
PBS	Phosphate buffered saline
PKM2	Pyruvate kinase isozyme typeM2
PLGA	Poly lactic-co-glycolic acid
SH2	Src homology domain 2
TAMs	Tumor associated macrophages
TIGIT	T cell immunoreceptor with Ig and ITIM domains
TIM3	T cell immunoglobulin domain and mucin domain-3
TGF-β	Transforming growth factor-β
TME	Tumor microenvironment
TNF-α	Tumor necrosis factor-α
Tregs	Regulatory T cells

Supplementary Information

Supplementary Material 1.

Author contributions
Zhenwei Song and Jian Zhang conceived and designed the experiments, and wrote the manuscript. Hongfei Chen and Yang Liu prepared Napabucasin-PLGA NPs and evaluated its Characterization. Xueyao Wang, Zhiyue Zhang, Hui Li, Huajun Zhao, Qiuju Han helped with the experimental setup and provided crucial suggestions for the manuscript.

Availability of data and materials
Not applicable.

Declarations

Ethics approval and consent to participate
All animal protocols and experiments were approved by the Institutional Animal Care and Use Committee of Shandong University, China, and complied with the Guide for the Care and Use of Laboratory Animals.

Consent for publication
All contributing authors agreed to the publication of this article.

Competing interests
The authors declare that they have no competing interests.

Author details
[1]Institute of Immunopharmaceutical Sciences, School of Pharmaceutical Sciences, Shandong University, Jinan, China. [2]NMPA Key Laboratory for Technology Research and Evaluation of Drug Products, Key Laboratory of Chemical Biology (Ministry of Education), Department of Pharmaceutics, School of Pharmaceutical Sciences, Cheeloo College of Medicine, Shandong University, Jinan 250012, China.

References

1. Fan Z, Zhou P, Jin B, Li G, Feng L, Zhuang C, Wang S. Recent therapeutics in hepatocellular carcinoma. Am J Cancer Res. 2023;13(1):261–75.
2. Kudo M, Finn RS, Qin S, Han KH, Ikeda K, Piscaglia F, Baron A, Park JW, Han G, Jassem J, et al. Lenvatinib versus sorafenib in first-line treatment of patients with unresectable hepatocellular carcinoma: a randomised phase 3 non-inferiority trial. Lancet. 2018;391(10126):1163–73.
3. Greten TF, Lai CW, Li G, Staveley-O'Carroll KF. Targeted and immune-based therapies for hepatocellular carcinoma. Gastroenterology. 2019;156(2):510–24.
4. Lee C, Cheung ST. STAT3: an emerging therapeutic target for hepatocellular carcinoma. Cancers. 2019;11(11):1646.
5. Taniguchi K, Karin M. NF-κB, inflammation, immunity and cancer: coming of age. Nat Rev Immunol. 2018;18(5):309–24.
6. Fan Y, Mao R, Yang J. NF-κB and STAT3 signaling pathways collaboratively link inflammation to cancer. Protein Cell. 2013;4(3):176–85.
7. Jin S, Yang X, Li J, Yang W, Ma H, Zhang Z. p53-targeted lincRNA-p21 acts as a tumor suppressor by inhibiting JAK2/STAT3 signaling pathways in head and neck squamous cell carcinoma. Mol Cancer. 2019;18(1):38.
8. Yang L, Lin S, Xu L, Lin J, Zhao C, Huang X. Novel activators and small-molecule inhibitors of STAT3 in cancer. Cytokine Growth Factor Rev. 2019;49:10–22.
9. Jonker DJ, Nott L, Yoshino T, Gill S, Shapiro J, Ohtsu A, Zalcberg J, Vickers MM, Wei AC, Gao Y, et al. Napabucasin versus placebo in refractory advanced colorectal cancer: a randomised phase 3 trial. Lancet Gastroenterol Hepatol. 2018;3(4):263–70.
10. Li Y, Han Q, Zhao H, Guo Q, Zhang J. Napabucasin reduces cancer stem cell characteristics in hepatocellular carcinoma. Front Pharmacol. 2020;11:597520.
11. Su Y, Zhang B, Sun R, Liu W, Zhu Q, Zhang X, Wang R, Chen C. PLGA-based biodegradable microspheres in drug delivery: recent advances in research and application. Drug Deliv. 2021;28(1):1397–418.
12. Grill AE, Shahani K, Koniar B, Panyam J. Chemopreventive efficacy of curcumin-loaded PLGA microparticles in a transgenic mouse model of HER-2-positive breast cancer. Drug Deliv Transl Res. 2018;8(2):329–41.
13. Zhang Z, Wang X, Li B, Hou Y, Yang J, Yi L. Development of a novel morphological paclitaxel-loaded PLGA microspheres for effective cancer therapy: in vitro and in vivo evaluations. Drug Deliv. 2018;25(1):166–77.
14. Shah SR, Kim J, Schiapparelli P, Vazquez-Ramos CA, Martinez-Gutierrez JC, Ruiz-Valls A, Inman K, Shamul JG, Green JJ, Quinones-Hinojosa A. Verteporfin-loaded polymeric microparticles for intratumoral treatment of brain cancer. Mol Pharm. 2019;16(4):1433–43.
15. DeNardo DG, Ruffell B. Macrophages as regulators of tumour immunity and immunotherapy. Nat Rev Immunol. 2019;19(6):369–82.
16. Pan Y, Yu Y, Wang X, Zhang T. Tumor-associated macrophages in tumor immunity. Front Immunol. 2020;11:583084.
17. Chen D, Zhang X, Li Z, Zhu B. Metabolic regulatory crosstalk between tumor microenvironment and tumor-associated macrophages. Theranostics. 2021;11(3):1016–30.
18. Fujiwara Y, Komohara Y, Kudo R, Tsurushima K, Ohnishi K, Ikeda T, Takeya M. Oleanolic acid inhibits macrophage differentiation into the M2 phenotype and glioblastoma cell proliferation by suppressing the activation of STAT3. Oncol Rep. 2011;26(6):1533–7.
19. Mohammadzadeh V, Norouzi A, Ghorbani M. Multifunctional nanocomposite based on lactose@layered double hydroxide-hydroxyapatite as a pH-sensitive system for targeted delivery of doxorubicin to liver cancer cells. Colloids Surf A. 2022;651: 129723.
20. Modi S, Anderson BD. Determination of drug release kinetics from nanoparticles: overcoming pitfalls of the dynamic dialysis method. Mol Pharm. 2013;10(8):3076–89.
21. Hubbard JM, Grothey A. Napabucasin: an update on the first-in-class cancer stemness inhibitor. Drugs. 2017;77(10):1091–103.

Song *et al. Journal of Translational Medicine*   (2024) 22:1125

Page 17 of 17

22. Chanmee T, Ontong P, Konno K, Itano N. Tumor-associated macrophages as major players in the tumor microenvironment. Cancers. 2014;6(3):1670–90.
23. Verdeil G, Lawrence T, Schmitt-Verhulst AM, Auphan-Anezin N. Targeting STAT3 and STAT5 in tumor-associated immune cells to improve immunotherapy. Cancers. 2019;11(12):1832.
24. Li X, Wenes M, Romero P, Huang SC, Fendt SM, Ho PC. Navigating metabolic pathways to enhance antitumour immunity and immunotherapy. Nat Rev Clin Oncol. 2019;16(7):425–41.
25. Remmerie A, Scott CL. Macrophages and lipid metabolism. Cell Immunol. 2018;330:27–42.
26. Alqahtani A, Khan Z, Alloghbi A, Said Ahmed TS, Ashraf M, Hammouda DM. Hepatocellular carcinoma: molecular mechanisms and targeted therapies. Medicina. 2019;55(9):526.
27. Liu Y, Fuchs J, Li C, Lin J. IL-6, a risk factor for hepatocellular carcinoma: FLLL32 inhibits IL-6-induced STAT3 phosphorylation in human hepatocellular cancer cells. Cell Cycle. 2010;9(17):3423–7.
28. He G, Yu GY, Temkin V, Ogata H, Kuntzen C, Sakurai T, Sieghart W, Peck-Radosavljevic M, Leffert HL, Karin M. Hepatocyte IKKbeta/NF-kappaB inhibits tumor promotion and progression by preventing oxidative stress-driven STAT3 activation. Cancer Cell. 2010;17(3):286–97.
29. He G, Karin M. NF-κB and STAT3—key players in liver inflammation and cancer. Cell Res. 2011;21(1):159–68.
30. Wang Z, Hui C, Xie Y. Natural STAT3 inhibitors: a mini perspective. Bioorg Chem. 2021;115: 105169.
31. Li Y, Rogoff HA, Keates S, Gao Y, Murikipudi S, Mikule K, Leggett D, Li W, Pardee AB, Li CJ. Suppression of cancer relapse and metastasis by inhibiting cancer stemness. Proc Natl Acad Sci USA. 2015;112(6):1839–44.
32. Pearce OMT, Delaine-Smith RM, Maniati E, Nichols S, Wang J, Böhm S, Rajeeve V, Ullah D, Chakravarty P, Jones RR, et al. Deconstruction of a metastatic tumor microenvironment reveals a common matrix response in human cancers. Cancer Discov. 2018;8(3):304–19.
33. Azizi E, Carr AJ, Plitas G, Cornish AE, Konopacki C, Prabhakaran S, Nainys J, Wu K, Kiseliovas V, Setty M, et al. Single-cell map of diverse immune phenotypes in the breast tumor microenvironment. Cell. 2018;174(5):1293-1308.e1236.
34. Martin JD, Cabral H, Stylianopoulos T, Jain RK. Improving cancer immunotherapy using nanomedicines: progress, opportunities and challenges. Nat Rev Clin Oncol. 2020;17(4):251–66.
35. Phuengkham H, Ren L, Shin IW, Lim YT. Nanoengineered immune niches for reprogramming the immunosuppressive tumor microenvironment and enhancing cancer immunotherapy. Adv Mater. 2019;31(34): e1803322.
36. Kortylewski M, Kujawski M, Wang T, Wei S, Zhang S, Pilon-Thomas S, Niu G, Kay H, Mulé J, Kerr WG, et al. Inhibiting Stat3 signaling in the hematopoietic system elicits multicomponent antitumor immunity. Nat Med. 2005;11(12):1314–21.
37. Herrmann A, Kortylewski M, Kujawski M, Zhang C, Reckamp K, Armstrong B, Wang L, Kowolik C, Deng J, Figlin R, et al. Targeting Stat3 in the myeloid compartment drastically improves the in vivo antitumor functions of adoptively transferred T cells. Cancer Res. 2010;70(19):7455–64.
38. Gotthardt D, Putz EM, Straka E, Kudweis P, Biaggio M, Poli V, Strobl B, Müller M, Sexl V. Loss of STAT3 in murine NK cells enhances NK cell-dependent tumor surveillance. Blood. 2014;124(15):2370–9.
39. Bied M, Ho WW, Ginhoux F, Blériot C. Roles of macrophages in tumor development: a spatiotemporal perspective. Cell Mol Immunol. 2023;20(9):983–92.
40. Eming SA, Murray PJ, Pearce EJ. Metabolic orchestration of the wound healing response. Cell Metab. 2021;33(9):1726–43.
41. Wang T, Liu H, Lian G, Zhang SY, Wang X, Jiang C. HIF1α-induced glycolysis metabolism is essential to the activation of inflammatory macrophages. Mediat Inflamm. 2017;2017:9029327.
42. Li Y, Song Z, Han Q, Zhao H, Pan Z, Lei Z, Zhang J. Targeted inhibition of STAT3 induces immunogenic cell death of hepatocellular carcinoma cells via glycolysis. Mol Oncol. 2022;16(15):2861–80.
43. Jiang Y, Han Q, Zhao H, Zhang J. Promotion of epithelial-mesenchymal transformation by hepatocellular carcinoma-educated macrophages through Wnt2b/β-catenin/c-Myc signaling and reprogramming glycolysis. J Exp Clin Cancer Res. 2021;40(1):13.
44. Van den Bossche J, O'Neill LA, Menon D. Macrophage immunometabolism: where are we (going)? Trends Immunol. 2017;38(6):395–406.
45. Andersen MN, Etzerodt A, Graversen JH, Holthof LC, Moestrup SK, Hokland M, Møller HJ. STAT3 inhibition specifically in human monocytes and macrophages by CD163-targeted corosolic acid-containing liposomes. Cancer Immunol Immunother. 2019;68(3):489–502.
46. Knochelmann HM, Dwyer CJ, Bailey SR, Amaya SM, Elston DM, Mazza-McCrann JM, Paulos CM. When worlds collide: Th17 and Treg cells in cancer and autoimmunity. Cell Mol Immunol. 2018;15(5):458–69.

Publisher's Note